Enhanced Iterative-based ZP-OFDM Receiver in Multi-Relay Cooperative Networks

Homa Eghbali, Ibrahim Abualhaol, and Sami Muhaidat

***Abstract*— Zero-Padding Orthogonal Frequency Division Multiplexing (ZP-OFDM) has recently been introduced to avoid coded-OFDM's high decoding complexity. Various sub-optimal ZP-OFDM receivers have been developed in the literature to tradeoff performance with implementation complexity. In this paper, we propose a new iterative detection scheme for ZP-OFDM transmissions tailored to broadband cooperative networks with multiple relays and amplify-and-forward relaying. By avoiding channel dependent matrix inversion, which is inevitable in the case of minimum mean square error (MMSE)-ZP-OFDM transmissions, and incorporating linear processing techniques, we show that our proposed low-complexity MMSE-ZP-OFDM (LC-MMSE-ZP-OFDM) receiver is able to bring significant complexity reduction in the receiver design, while outperforming cooperative MMSE-ZP-OFDM. Thorough computational complexity analysis for LC-MMSE-ZP-OFDM and D-MMSE-ZP-OFDM receivers is presented. Furthemore, an extensive Monte Carlo simulation study is provided to corroborate the analytical results and to provide detailed performance comparison between LC-MMSE-ZP-OFDM and D-MMSE-ZP-OFDM receivers with/without error prapogation.**

***Index Terms*—Cooperative communication, Zero-Padding orthogonal frequency division multiplexing, Equalization.**

I. Introduction

Due to the increasing demand for high speed data communication, intensive research efforts have been done on this area. The dispersive nature of the frequency selective fading channels causes intersymbol interference (ISI), which in turn incurs high performance degradation. This phenomenon is the key challenge for high-speed broadband applications. Orthogonal Frequency Division Multiplexing (OFDM) was proposed as an efficient technique to mitigate ISI. In OFDM transmission, the ISI channel with additive white Gaussian noise (AWGN) is converted into parallel ISI-free subchannels by implementing Inverse Fast Fourier Transform (IFFT) at the transmitter and Fast Fourier Transform (FFT) at the receiver side [1]. OFDM is an attractive equalization scheme for digital audio broadcasting (DAB) and digital video broadcasting (DBV) [2]-[3], and has successfully been applied to high-speed modems over digital subscriber lines (xDSL) [4], and recently has also been proposed for broadband television systems and mobile wireless local area networks such as IEEE802.11a and HIPERLAN/2 (HL2) standards [5].

OFDM is capable of very simple equalization of frequency selective finite impulse response (FIR) channels, by applying the IFFT precoding at the transmitter side and cyclic prefix (CP) insertion. The CP is then discarded to avoid inter block interfernce (IBI) between successive blocks and the truncated blocks are further FFT processed to convert the linear channel convolution into circular convolution. In this way the receiver complexity in both equalization and the symbol decoding stages is reduced [6]. Nevertheless, each data symbol is sent over a single flat fading subchannel and the underlying multipath diversity is lost. Moreover, there is no guarantee for symbol detectability when channel nulls happen in the subchannels which causes performance loss. At the expense of bandwidth overexpansion, the fading resilient coded OFDM (C-OFDM) [8] was proposed, ameliorating the incurred performance losses by subchannel nulls. To deal with such diversity losses, error control codes such as Trellis-coded modulation (TCM) [7], and convolutional codes [9] were suggested to be invoked before the IFFT processing. Interleaving together with TCM enjoys low complexity Viterbi decoding while enabling a better trade off between bandwidth and efficiency. However, designing systems that achieve diversity gain equal to code length is difficult considering TCM's standard design paradigms. As an alternative to various error-control coding techniques, linear constellation precoded OFDM (LCP-OFDM) was proposed [10] which linearly precodes symbols before they are multiplexed. The real orthogonal precoder in LCP is applied to maximize the minimum product distance [11]-[12] and channel cutoff rate [13], while maintaining the transmission rate and guaranteeing the symbol recovery. To enable the maximum possible diversity and coding gain, subcarrier grouping was proposed [10]. However, the LCP that is used within each subset of subcarriers is in general complex.

Zero-Padding (ZP) of multicarrier transmission has been proposed, replacing the generally non-zero CP, to ensure symbol recovery regardless of channel nulls. ZP-OFDM guarantees symbol recovery and FIR equalization of FIR channels, which is not the case for CP-OFDM. By appending the zero symbols after the IFFT processed information symbols in ZP-OFDM, the single FFT required by CP-OFDM is replaced by FIR filtering in ZP-OFDM which adds to the

H. Eghbali and S. Muhaidat are with the School of Engineering Science, Simon Fraser University, Burnaby, B.C., Canada (e-mail: homa.eghbali@ieee.org, muhaidat@ieee.org). I. Abualhaol is an assistant professor at Khalifa University of Science, Technology, and Research, Sharjah, United Arab Emirates (e-mail: ibrahimee@ieee.org).

receiver complexity. Two low complexity equalizers for ZP-OFDM were proposed in [14] to tradeoff performance with implementation complexity.

To reap the benefits of multiple-input multiple-output (MIMO) communications in a wireless scenario with single antenna terminals, cooperative diversity [15] was proposed as an alternative to multiple-antenna transmission schemes. Cooperative diversity provides an effective means of improving spectral and power efficiency of wireless networks [16]-[20]. In cooperative diversity, the signal transmitted by the source node is overheard by other nodes, also defined as partners. The source and its partners can jointly process and transmit their information, creating a ``virtual antenna array", although each of them is equipped with only one antenna. Basic cooperation protocols can be used with either amplify-and-forward (AF) or decode-and-forward (DF) relaying.

OFDM has been recently applied to cooperative communication. Specifically, OFDM-based multihop relaying has been studied in [21]-[24]. The integration of receive diversity (RD), transmit diversity (TD), and simplified transmit diversity (STD) protocols with OFDM has also been studied in the literature [26] and [27]. These works, however, are mainly limited to single relay scenarios.

In this paper, we propose a novel iterative detection scheme for multi-relay cooperative ZP-OFDM transmissions with AF relaying, that is not only outperforms cooperative MMSE-ZP-OFDM, but also uses low-complexity computational methods by avoiding inversion of *channel dependent matrices*, which brings a significant power saving to the LC-MMSE-ZP-OFDM receiver. This makes the LC-MMSE-ZP-OFDM receiver a strong candidate for wireless sensor networks (WSNs) that are characterized by small and low-power devices. We show that by applying low-complexity linear processing techniques, the LC-MMSE-ZP-OFDM receiver is able to collect both multipath and spatial diversity gains, leading to significant improvement in performance.

The rest of this paper is organized as follows. We start in Section II by describing our model and assumptions. In Section III, the efficient iterative receiver is proposed. Computational complexity analysis and numerical results are presented in Section IV and Section V, respectively. The paper is concluded in Section VI.

Notation: $\bar{(.)}, (.)^{\mathrm{T}}, (.)^{\dagger}$ and $(.)^{\mathrm{H}}$ denote conjugate, transpose, pseudo inverse and Hermitian transpose operations, respectively. * denotes linear convolution, $|.|$ denotes the absolute value, and $\|.\|$ denotes the Euclidean norm of a vector. $[.]_{k,l}$ denotes the $(k,l)^{th}$ entry of a matrix, $[.]_k$ denotes the k^{th} entry of a vector, $\mathbf{I}_M$ denotes the identity matrix of size M, and $\mathbf{0}_{M\times M}$ denotes all-zero matrix of size $M\times M$. $\mathbf{Q}_M^{-1}=\mathbf{Q}_M^H$ represents the $M\times M$ IFFT matrix whose $(k,l)^{th}$ element is given by $\mathbf{Q}(k,l)=1/\sqrt{M}\exp(j2\pi kl/M)$ where $0\le k,l\le M-1$. $E_i[.]$ and $\Gamma[.]$ represent the exponential-integral function and the gamma function, respectively [30] Bold upper-case letters denote matrices and bold lower-case letters denote vectors.

II. System and Channel Models

We consider a multiple-relay assisted cooperative wireless communication system with a single source (S), N_R half-duplex relay terminals (R_i), $i=1,2,...,N_R$, and a single destination (D). The source, destination, and all relays are equipped with single transmit and receive antennas. Any linear modulation technique such as QAM or PSK can be used. We assume the AF relaying and adopt the user cooperation protocol proposed by Nabar *et al.* [25]. Specifically, in the broadcasting phase, the source node transmits to the relay nodes and the destination node. In the relaying phase, the relay nodes forward a scaled noisy version of the received signal to the destination node.

The relay assisted ZP-OFDM transmission is illustrated in Fig. 1. The channel impulse responses (CIRs) for $S\to R_i$, $S\to D$, and $R_i\to D$ links for the i^{th} relay terminal and j^{th} transmission block are given by $\mathbf{h}_{SR_i}^j=\left[h_{SR_i}^j[0],...,h_{SR}^j[L_{SR_i}]\right]^{\mathrm{T}}$, $\mathbf{h}_{SD}^j=\left[h_{SD}^j[0],...,h_{SD}^j[L_{SD}]\right]^{\mathrm{T}}$ and $\mathbf{h}_{R_iD}^j=\left[h_{R_iD}^j[0],...,h_{R_iD}^j[L_{R_iD}]\right]^{\mathrm{T}}$, respectively, where L_{SR_i}, L_{SD}, and L_{R_iD} denote the corresponding channel memory lengths. All $S\to R_i$, $S\to D$, and $R_i\to D$ links are assumed to experience frequency selective Rayleigh fading. The random vectors $\mathbf{h}_{SR_i}$, $\mathbf{h}_{SD}$, and $\mathbf{h}_{R_iD}$ are assumed to be independent zero-mean complex Gaussian with power delay profile vectors denoted by $\mathbf{v}_{SR_i}=[\sigma_{SR_i}^2(0),...,\sigma_{SR_i}^2(L_{SR_i})]$, $\mathbf{v}_{SD}=[\sigma_{SD}^2(0),...,\sigma_{SD}^2(L_{SD})]$, and $\mathbf{v}_{R_iD}=[\sigma_{R_iD}^2(0),...,\sigma_{R_iD}^2(L_{R_iD})]$ that are normalized such that $\sum_{l_{SR_i}=0}^{L_{SR_i}}\sigma_{SR_i}^2(l_{SR_i})=1$, $\sum_{l_{SD}=0}^{L_{SD}}\sigma_{SD}^2(l_{SD})=1$, and $\sum_{l_{R_iD}=0}^{L_{R_iD}}\sigma_{R_iD}^2(l_{R_iD})=1$. The j^{th} $M\times 1$ information block $\mathbf{x}_M^j$ is padded by β trailing zeros where $\beta=\max(L_{SD},L_{SR_i}+L_{R_iD}+1)$ and IFFT precoded by the IFFT matrix to yield the time-domain block vector $\mathbf{x}_{zp}^j$

$$\mathbf{x}_{zp}^j=\mathbf{Q}_{zp}\mathbf{x}_M^j, \tag{1}$$

where

$$\mathbf{Q}_{zp}=[\mathbf{Q}_M\ \mathbf{0}_{\beta\times M}]^H. \tag{2}$$

and $\mathbf{Q}_M$ represents the $M\times M$ FFT matrix. The signal received at the i^{th} relay terminal during the broadcasting phase is

$$\mathbf{r}_{R_i}^j=\sqrt{E_{SR_i}}\mathbf{H}_{SR_i}\mathbf{Q}_{zp}\mathbf{x}_M^j+\sqrt{E_{SR_i}}\mathbf{H}_{SR_i-IBI}\mathbf{Q}_{zp}\mathbf{x}_M^{j-1}+\mathbf{n}_{R_i}^j, \tag{3}$$

where $N = M + \beta$, E_{SR_i} is the average signal energy over one symbol period received at i^{th} relay terminal, $\mathbf{H}_{SR_i}$ is the $N \times N$ lower triangular Toeplitz filtering matrix with its first column being $\left[h^j_{SR_i}[0],...,h^j_{SR_i}[L_{SR_i}] \;\; 0,...,0\right]^{\mathrm{T}}$, $\mathbf{H}_{SR_i-IBI}$ is the $N \times N$ upper triangular Toeplitz filtering matrix that captures the inter-block interference (*IBI*) with its first row being $\left[0,...,0 \;\; h^j_{SR_i}[0],...,h^j_{SR_i}[L_{SR_i}]\right]$, and $\mathbf{n}^j_{R_i}$ is the additive white Gaussian noise vector with each entry having zero-mean and variance of $N_0/2$ per dimension. Having $\mathbf{H}_{SR_i-IBI}\mathbf{Q}_{zp} = 0$, the all-zero $\mathbf{0}_{\beta \times M}$ matrix plays the key role in ZP-OFDM by eliminating the *IBI*. Having the $\mathbf{H}_{SR_i}$ matrix partitioned between its first M and last β columns as $\mathbf{H}_{SR_i} = [\mathbf{H}_{SR_i-0}, \mathbf{H}_{SR_i-zp}]$, the received block symbol at the relay terminal during the broadcasting phase will be given by

$$\mathbf{r}^j_{R_i} = \sqrt{E_{SR_i}}\mathbf{H}_{SR_i}\mathbf{Q}_{zp}\mathbf{x}^j_M + \mathbf{n}^j_{R_i} = \sqrt{E_{SR_i}}\mathbf{H}_{SR_i-0}\mathbf{Q}^H_M\mathbf{x}^j_M + \mathbf{n}^j_{R_i}. \quad (4)$$

The $N \times M$ submatrix $\mathbf{H}_{SR_i-0}$, which corresponds to the first M columns of $\mathbf{H}_{SR_i}$, is Toeplitz and is guaranteed to be invertible, which assures symbol recovery regardless of channel zero locations.

The signal received at the destination during the broadcasting phase is

$$\mathbf{r}^j_{D,1} = \sqrt{E_{SD}}\mathbf{H}_{SD}\mathbf{Q}_{zp}\mathbf{x}^j_M + \sqrt{E_{SD}}\mathbf{H}_{SD-IBI}\mathbf{Q}_{zp}\mathbf{x}^{j-1}_M + \mathbf{n}^j_{D,1}, \quad (5)$$

where E_{SD} is the average signal energy over one symbol period received at the destination terminal, $\mathbf{H}_{SD}$ is the $N \times N$ lower triangular Toeplitz filtering matrix with its first column being $\left[h^j_{SD}[0],...,h^j_{SD}[L_{SD}] \;\; 0,...,0\right]^{\mathrm{T}}$, $\mathbf{H}_{SD-IBI}$ is the $N \times N$ upper triangular Toeplitz filtering matrix that captures *IBI* with its first row being $\left[0,...,0 \;\; h^j_{SD}[0],...,h^j_{SD}[L_{SD}]\right]$, and $\mathbf{n}^j_{D,1}$ is the additive white Gaussian noise vector with each entry having zero-mean and variance of $N_0/2$ per dimension. Following similar simplification applied in (4), (5) can be written as

$$\mathbf{r}^j_{D,1} = \sqrt{E_{SD}}\mathbf{H}_{SD}\mathbf{Q}_{zp}\mathbf{x}^j_M + \mathbf{n}^j_{D,1} = \sqrt{E_{SD}}\mathbf{H}_{SD-0}\mathbf{Q}^H_M\mathbf{x}^j_M + \mathbf{n}^j_{D,1}. \quad (6)$$

To ensure that the power budget is not violated, the relay terminals normalize each entry of the respective received signal $[\mathbf{r}^j_{R_i}]_n$, $n = 1,2,...,N$, by a factor of $\mathrm{E}\left(|[\mathbf{r}^j_{R_i}]_n|^2\right) = E_{SR_i} + N_0$ to ensure unit average energy and retransmits the signal during the relaying phase. After some mathematical manipulations, the received signal at the destination terminal during the relaying phase is given by

$$\begin{aligned}\mathbf{r}^j_{D,2} &= \sum_{i=1}^{N_R}\sqrt{\frac{E_{R_iD}E_{SR_i}}{E_{SR_i}+N_0}}\mathbf{H}_{SR_iD}\mathbf{Q}_{zp}\mathbf{x}^j_M + \mathbf{n}^j_{D,2} \\ &= \sum_{i=1}^{N_R}\sqrt{\frac{E_{R_iD}E_{SR_i}}{E_{SR_i}+N_0}}\mathbf{H}_{SR_iD-0}\mathbf{Q}^H_M\mathbf{x}^j_M + \mathbf{n}^j_{D,2},\end{aligned} \quad (7)$$

where $\mathbf{H}_{SR_iD}$ is the $N \times N$ lower triangular Toeplitz filtering matrix with its first column being $\left[h^j_{SR_iD}[0],...,h^j_{SR_iD}[L_{SR_iD}] \;\; 0,...,0\right]^{\mathrm{T}}$, $\mathbf{h}_{SR_iD} = \mathbf{h}_{R_iD} * \mathbf{h}_{SR_i}$, $L_{SR_iD} = L_{SR_i} + L_{R_iD} + 1$, $\mathbf{H}_{SR_iD-0}$ is the first M columns of $\mathbf{H}_{SR_iD}$, and $\mathbf{n}^j_{D,2}$ is conditionally (conditioned on $\mathbf{h}_{R_iD}$) complex Gaussian with zero mean and variance $\sigma^2_n = N_0\left(1 + \sum_{i=1}^{N_R}\frac{E_{R_iD}}{E_{SR_i}+N_0}\sum_{l=0}^{L_{R_iD}}\left|\mathbf{h}^j_{R_iD}(l)\right|^2\right)$.

Assuming unity variance $\sigma^2_x = 1$ for the symbols, the decoded signals using the MMSE equalizer are given by

$$\mathbf{z}_{mmse} = \sqrt{E_{SD}}\mathbf{Q}_M\mathbf{H}^H_{SD-0}\mathbf{B}\mathbf{r}^j_{D,1} + \sum_{i=1}^{N_R}\sqrt{\frac{E_{R_iD}E_{SR_i}}{E_{SR_i}+N_0}}\mathbf{Q}_M\mathbf{H}^H_{SR_iD-0}\mathbf{B}\mathbf{r}^j_{D,2}, \quad (8)$$

where

$$\begin{aligned}\mathbf{B} = [&(\sigma^2_n + N_0)\mathbf{I_N} + E_{SD}\mathbf{H^H_{SD-0}}\mathbf{H_{SD-0}} \\ &+ \sum_{i=1}^{N_R}\frac{E_{R_iD}E_{SR_i}}{E_{SR_i}+N_0}\mathbf{H^H_{SR_iD-0}}\mathbf{H_{SR_iD-0}}]^{-1}.\end{aligned} \quad (9)$$

Note that to perform MMSE equalization, inverse of a channel dependent $N \times N$ matrix should be precomputed which brings an extra implementation cost for the D-MMSE-ZP-OFDM receiver. To overcome this limitation, our proposed scheme targets practical D-MMSE-ZP-OFDM receiver that exploits full multipath diversity while maintaining much lower complexity.

III. The Efficient Iterative System

The LC-MMSE-ZP-OFDM receiver shown in Fig. 2 includes a suboptimal channel independent MMSE equalizer in the feed forward stage, followed by linear processing operations in the feed-back stage. Specifically, the feed forward stage exploits the circulant structure of the channel matrices,

$$\begin{aligned}\mathbf{H}'_{SR_iD} &= \mathbf{Q}\Lambda_{SR_iD}\mathbf{Q}^H, \\ \mathbf{H}'_{SD} &= \mathbf{Q}\Lambda_{SD}\mathbf{Q}^H,\end{aligned} \quad (10)$$

where $\mathbf{H}'_{SR_iD}$ and $\mathbf{H}'_{SD}$ are $N \times N$ circulant matrices with entries $[\mathbf{H}'_{SR_iD}]_{k,l} = \mathbf{h}_{SR_iD}((k-l)\bmod N)$ and $[\mathbf{H}'_{SD}]_{k,l} = \mathbf{h}_{SD}((k-l)\bmod N)$. $\mathbf{\Lambda}_{SR_iD}$ and $\mathbf{\Lambda}_{SD}$ are diagonal matrices whose $(n,n)^{th}$ elements are equal to the n^{th} DFT coefficients of $\mathbf{h}_{SR_iD}$ and $\mathbf{h}_{SD}$, respectively. Due to the trailing zeros, the last β columns of $\mathbf{H}_{SD}$ and $\mathbf{H}_{SR_iD}$ in (6) and (7) do not affect the received block. Thus, the Toeplitz matrices $\mathbf{H}_{SD}$ and $\mathbf{H}_{SR_iD}$ can be replaced by the $N \times N$ circulant matrices $\mathbf{H}'_{SD}$ and $\mathbf{H}'_{SR_iD}$ and (6) and (7) can be written as

$$\begin{aligned}\mathbf{r}_{D,1}^{j} &= \sqrt{E_{SD}}\mathbf{H}'_{SD}\mathbf{Q}_{zp}\mathbf{x}_M^j + \mathbf{n}_{D,1}^{j},\\ \mathbf{r}_{D,2}^{j} &= \sum_{i=1}^{N_R}\sqrt{\frac{E_{R_iD}E_{SR_i}}{E_{SR_i}+N_0}}\mathbf{H}'_{SR_iD}\mathbf{Q}_{zp}\mathbf{x}_M^j + \mathbf{n}_{D,2}^{j}.\end{aligned} \tag{11}$$

$\mathbf{H}'_{SD}$ and $\mathbf{H}'_{SR_iD}$ matrices take advantage of FFT to yield a set of flat fading channels that can be equalized easily. Therefore, (11) can be rewritten as following

$$\begin{aligned}\mathbf{r}_{D,1}^{j} &= \sqrt{E_{SD}}\mathbf{Q}_N\mathbf{H}'_{SD}\mathbf{Q}_{zp}\mathbf{x}_M^j + \mathbf{n}_{D,1}^{j}\\ &= \sqrt{E_{SD}}\mathbf{Q}_N\mathbf{H}'_{SD}\mathbf{Q}_N^H\mathbf{Q}_N\mathbf{Q}_{zp}\mathbf{x}_M^j + \mathbf{n}_{D,1}^{j}\\ &= \sqrt{E_{SD}}\Lambda_{SD}\mathbf{Q}_N\mathbf{Q}_{zp}\mathbf{x}_M^j + \mathbf{n}_{D,1}^{j}\\ &= \sqrt{E_{SD}}\Lambda_{SD}\mathbf{V}\mathbf{x}_M^j + \mathbf{n}_{D,1}^{j},\end{aligned} \tag{12}$$

$$\mathbf{r}_{D,2}^{j} = \sum_{i=1}^{N_R}\sqrt{\frac{E_{R_iD}E_{SR_i}}{E_{SR_i}+N_0}}\Lambda_{SR_iD}\mathbf{V}\mathbf{x}_M^j + \mathbf{n}_{D,2}^{j}, \tag{13}$$

where

$$\mathbf{V} = \mathbf{Q}_N\mathbf{Q}_{zp}. \tag{14}$$

Having this, the suboptimal D-MMSE-ZP-OFDM receiver in the feed forward stage is formed in two steps. First, following [14], we obtain an MMSE estimator of $\mathbf{y}_N^j = \mathbf{V}\mathbf{x}_M^j$ using

$$\hat{\mathbf{y}}_N^j = E[\mathbf{y}_N^j(\mathbf{r}^j)^H].E^{-1}[\mathbf{r}^j(\mathbf{r}^j)^H]\mathbf{r}^j =$$

$$\mathbf{V}\mathbf{V}^H\left(\sqrt{E_{SD}}\Lambda_{SD} + \sum_{i=1}^{N_R}\sqrt{\frac{E_{R_iD}E_{SR_i}}{E_{SR_i}+N_0}}\Lambda_{SR_iD}\right)^H \times \tag{15}$$

$$\left[\begin{array}{c}(\sigma_n^2+N_0)\mathbf{I}_N + \\ \left\{\left(\sqrt{E_{SD}}\Lambda_{SD} + \sum_{i=1}^{N_R}\sqrt{\frac{E_{R_iD}E_{SR_i}}{E_{SR_i}+N_0}}\Lambda_{SR_iD}\right)\mathbf{V}\mathbf{V}^H \times \right. \\ \left.\left(\sqrt{E_{SD}}\Lambda_{SD} + \sum_{i=1}^{N_R}\sqrt{\frac{E_{R_iD}E_{SR_i}}{E_{SR_i}+N_0}}\Lambda_{SR_iD}\right)^H\right\}\end{array}\right]^{-1}\mathbf{r}^j,$$

where $\mathbf{r}^j = \mathbf{r}_{D,1}^j + \mathbf{r}_{D,2}^j$. The $(m,n)^{th}$ element of $\mathbf{V}\mathbf{V}^H$ is equivalent to $\frac{1}{N}\left\{\frac{1-e^{j2\pi(n-m)(M+1)/N}}{1-e^{j2\pi(n-m)/N}}-1\right\}$. Therefore, (15) can be further simplified assuming that $\mathbf{V}\mathbf{V}^H \approx M/N\,\mathbf{I}$, leading to

$$\hat{\mathbf{y}}_N^j = \left(\sqrt{E_{SD}}\Lambda_{SD} + \sum_{i=1}^{N_R}\sqrt{\frac{E_{R_iD}E_{SR_i}}{E_{SR_i}+N_0}}\Lambda_{SR_iD}\right)^H \times$$

$$\left[\begin{array}{c}\frac{N}{M}(\sigma_n^2+N_0)\mathbf{I}_N + \\ \left\{\left(\sqrt{E_{SD}}\Lambda_{SD} + \sum_{i=1}^{N_R}\sqrt{\frac{E_{R_iD}E_{SR_i}}{E_{SR_i}+N_0}}\Lambda_{SR_iD}\right)\times \right. \\ \left.\left(\sqrt{E_{SD}}\Lambda_{SD} + \sum_{i=1}^{N_R}\sqrt{\frac{E_{R_iD}E_{SR_i}}{E_{SR_i}+N_0}}\Lambda_{SR_iD}\right)^H\right\}\end{array}\right]^{-1}\mathbf{r}^j. \tag{16}$$

(16)

The resulting data streams detected from (16) are fed into a minimum Euclidean distance decoder, yielding $\hat{\mathbf{x}}_M^j$, (i.e., a decoded version of the transmitted symbols).

The decoded signals are then fed into the feed-back stage, which is responsible for exploiting the underlying multipath diversity. Specifically, consider the generation of the matrix Π_l, $l = 0,1,2,...,L$, as follows:

$$\begin{aligned}&\left[\Pi_{SR_iD,l}\right]_{p,q}, l = 1,...,L_{SR_i}+L_{R_iD}+1\\ &= \begin{cases}0 & p-q\bmod N = l\\ \left[\mathbf{H}'_{R_iD}\mathbf{H}'_{SR_i}\right]_{p,q} & p-q\bmod N \neq l'\end{cases}\\ &\left[\Pi_{SD,l}\right]_{p,q}, l = 1,...,L_{SD}+1\\ &= \begin{cases}0 & p-q\bmod N = l\\ \left[\mathbf{H}'_{SD}\right]_{p,q} & p-q\bmod N \neq l'\end{cases}\end{aligned} \tag{17}$$

$\left[\Pi_{SD,l}\right]_{p,q}, l = L_{SD}+2,...,L_{SR}+L_{RD}+1 = \left[\mathbf{H}'_{SD}\right]_{p,q}$,

where , $q \le N$, $[\mathbf{H}'_{SR_i}]_{k,l} = \mathbf{h}_{SR_i}((k-l)\bmod N)$, and $[\mathbf{H}'_{R_iD}]_{k,l} = \mathbf{h}_{R_iD}((k-l)\bmod N)$. Thus, (6) and (7) can be re-written as

$$\begin{aligned}\mathbf{r}'_{D1,l} &= \mathbf{r}_{D,1}^j - \sqrt{E_{SD}}\Pi_{SD,l}\mathbf{Q}_{zp}\hat{\mathbf{x}}_M^j,\\ \mathbf{r}'_{D2,l} &= \mathbf{r}_{D,2}^j - \sum_{i=1}^{R}\sqrt{\frac{E_{R_iD}E_{SR_i}}{E_{SR_i}+N_0}}\Pi_{SR_iD,l}\mathbf{Q}_{zp}\hat{\mathbf{x}}_M^j.\end{aligned} \tag{18}$$

Decision feedback equalizers normally operate at the relatively high SNR, so that the probability of decision error is [33]. Under the high SNR assumption, we can safely assume that $\hat{\mathbf{x}}_M^j \approx \mathbf{x}_M^j$. Therefore, we can write (18) as follows:

$$\begin{aligned}\mathbf{r}'_{D1,l} &= \sqrt{E_{SD}}\mathbf{P}_{SD,l}\mathbf{Q}_{zp}\hat{\mathbf{x}}_M^j,\\ \mathbf{r}'_{D2,l} &= \sum_{i=1}^{R}\sqrt{\frac{E_{R_iD}E_{SR_i}}{E_{SR_i}+N_0}}\mathbf{P}_{SR_iD,l}\mathbf{Q}_{zp}\hat{\mathbf{x}}_M^j,\end{aligned} \tag{19}$$

where $\mathbf{r}_{D,1}^j$ and $\mathbf{r}_{D,2}^j$ are the received signals as given in (6) and (7) and $\mathbf{P}_{SD,l}$ and $\mathbf{P}_{SR_iD,l}$ are given as

$$\begin{aligned}&\left[\mathbf{P}_{SR_iD,l}\right]_{p,q}, \quad l = 1,...,L_{SR}+L_{RD}+1 =\\ &\begin{cases}\left[\mathbf{H}'_{R_iD}\mathbf{H}'_{SR_i}\right]_{p,q} & p-q\bmod N = l\\ 0 & p-q\bmod N \neq l\end{cases},\\ &\left[\mathbf{P}_{SD,l}\right]_{p,q}, \quad l = 1,...,L_{SD}+1 =\\ &\begin{cases}\left[\mathbf{H}'_{SD}\right]_{p,q} & p-q\bmod N = l\\ 0 & p-q\bmod N \neq l\end{cases},\\ &\left[\mathbf{P}_{SD,l}\right]_{p,q}, \quad l = L_{SD}+2,...,L_{SR}+L_{RD}+1 = 0.\end{aligned} \tag{20}$$

For each diversity branch we have

$$\mathbf{r}''_{D1,l} = \sqrt{E_{SD}}(\mathbf{P}_{SD,l})^H \mathbf{r}_{D1,l} = E_{SD}\left\|\mathbf{P}_{SD,l}\right\|^2 \mathbf{Q}_{zp}\hat{\mathbf{x}}_M^j,$$

$$\mathbf{r}''_{D2,l} = \sum_{i=1}^{N_R}\sqrt{\frac{E_{R_iD}E_{SR_i}}{E_{SR_i}+N_0}}(\mathbf{P}_{SR_iD,l})^H \mathbf{r}_{D2,l} = \sum_{i=1}^{N_R}\frac{E_{R_iD}E_{SR_i}}{E_{SR_i}+N_0}\left\|\mathbf{P}_{SR_iD,l}\right\|^2 \mathbf{Q}_{zp}\hat{\mathbf{x}}_M^j. \quad (21)$$

The output streams in (21) are then combined resulting in

$$\frac{(\mathbf{Q}_{zp})^H}{\sum_{l=0}^{L}\left(E_{SD}\left\|\mathbf{P}_{SD,l}\right\|^2 + \sum_{i=1}^{N_R}\frac{E_{R_iD}E_{SR_i}}{E_{SR_i}+N_0}\left\|\mathbf{P}_{SR_iD,l}\right\|^2\right)}\sum_{l=0}^{L}\left(\mathbf{r}''_{D1,l}+\mathbf{r}''_{D2,l}\right), \quad (22)$$

where $L = L_{SR} + L_{RD} + 1$ assuming that $L_{SD} < L$. The scenario where $L_{SD} > L$ can be treated similarly. The signal in (22) is then fed into a maximum likelihood decoder to recover the transmitted symbols.

IV. Computational Complexity Analysis

In this section, we focus on the computational complexity of the LC-MMSE-ZP-OFDM receiver compared to the conventional D-MMSE-ZP-OFDM receiver. The computational complexity is measured based on the number of the complex multiplications and divisions. Since Complex divisions can be implemented in various different ways, we did not decompose them into complex multiplication. The overall computational complexity for the LC-MMSE-ZP-OFDM receiver and the conventional D-MMSE-ZP-OFDM receiver are summarized in Table I for the existing HL2 OFDM system and scenarios with different combinations of channel memory lengths with 10 relays present:

Scenario 1) $L_{SR_i} = L_{R_iD} = 2, L_{SD} = 4, i = 1,...,10$

Scenario 2) $L_{SR_i} = 4, L_{R_iD} = 3, L_{SD} = 7, i = 1,...,10$

Scenario 3) $L_{SR_i} = L_{R_iD} = 5, L_{SD} = 10, i = 1,...,10.$

Note that its not trivial to elaborate explicit complexity expressions for different OFDM systems in terms of the system's parameters. Specifically, in this work, we have used Matlab simulations to find the exact complexity figures. To do so, we have used the minimal multiplicative bounds [31] to find the arithmetic complexity of FFT of different block lengths. Besides, to implement the FFT of length W decomposable to the product of two prime numbers a and b, we have implemented a FFTs of size b or b FFTs of size a instead, without inquiring any additional operations such as multiplications by twiddle factors [32]. The computational complexity of the LC-MMSE-ZP-OFDM receiver versus the D-MMSE-ZP-OFDM receiver in terms of the number of the complex multiplications, is illustrated in Fig. 3, which is plotted against time, assuming that the channel estimate is updated at every t seconds. We would like to emphasize that the MMSE equalizer in D-MMSE-ZP-OFDM requires the inversion of an $N \times N$ Toeplitz channel dependent matrix, which has to be computed at every t seconds with a complexity of the order $O(N^2)$. Note that as the channel memory lengths of the underlying channel links increase, the complexity of both D-MMSE-ZP-OFDM and the LC-MMSE-ZP-OFDM receiver increases. However, as the number of participating relays increases, the complexity of the LC-MMSE-ZP-OFDM receiver stays unchanged, while the complexity of the D-MMSE-ZP-OFDM receiver increases. Therefore, our LC-MMSE-ZP-OFDM receiver is an ideal choice for systems with a larger number of relays.

It is observed from Fig. 3 that for scenarios one and two with reasonable memory length for the underlying channels, the aggregate complexity of the LC-MMSE-ZP-OFDM receiver is insignificant compared to the conventional MMSE-ZP-OFDM, as channel parameters change with time.

V. Numerical Results

In this section, we present Monte-Carlo simulation results for the LC-MMSE-ZP-OFDM receiver assuming a quasi-static Rayleigh fading channel for the $S \to R$, $R \to D$, and $S \to D$ links. We assume 16-PSK modulation.

First, we assume that there are two relay nodes, where each node is equipped with one antenna. We set $E_{R_1D} = E_{R_2D} = 10$ dB and the SER curve is plotted against E_{SD}/N_0. The scenarios with different combinations of channel memory lengths are considered:

Scenario 1) $L_{SR_1} = 0, L_{R_1D} = 0, L_{SR_2} = 0, L_{R_2D} = 0, L_{SD} = 0,$

Scenario 2) $L_{SR_1} = 0, L_{R_1D} = 1, L_{SR_2} = 0, L_{R_2D} = 0, L_{SD} = 0,$

Scenario 3) $L_{SR_1} = 0, L_{R_1D} = 2, L_{SR_2} = 0, L_{R_2D} = 1, L_{SD} = 0,$

Scenario 4) $L_{SR_1} = 1, L_{R_1D} = 1, L_{SR_2} = 0, L_{R_2D} = 0, L_{SD} = 0,$

Scenario 5) $L_{SR_1} = 2, L_{R_1D} = 1, L_{SR_2} = 1, L_{R_2D} = 0, L_{SD} = 0,$

Scenario 6) $L_{SR_1} = 3, L_{R_1D} = 1, L_{SR_2} = 2, L_{R_2D} = 0, L_{SD} = 0.$

As can be noticed from Fig. 4, the SER curves for the first three scenarios have identical slopes for high E_{SD}/N_0 values, achieving the full diversity order of $L_{SD} + 1 + \sum_{i=1}^{2}\left(\min(L_{SR_i}, L_{R_iD}) + 1\right) = 3$, as predicted. The second three curves have identical slopes similarly, achieving the full diversity order of $L_{SD} + 1 + \sum_{i=1}^{2}\left(\min(L_{SR_i}, L_{R_iD}) + 1\right) = 4$.

Secondly, we assume that there are three relay nodes, where each node is equipped with one antenna. We set $E_{R_1D} = E_{R_2D} = E_{R_3D} = 10$ dB, and the SER curve is plotted against E_{SD}/N_0. The scenarios with different combinations of channel memory lengths are considered:

Scenario1) $L_{SR_1} = L_{R_1D} = L_{SR_2} = L_{R_2D} = L_{SR_3} = L_{R_3D} = L_{SD} = 0,$

Scenario2) $L_{SD} = L_{SR_1} = L_{SR_2} = L_{SR_3} = 0, L_{R_1D} = L_{R_2D} = L_{R_3D} = 1,$

Scenario3) $L_{SR_1} = L_{R_1D} = L_{SR_2} = 1, L_{SD} = L_{R_2D} = L_{SR_3} = L_{R_3D} = 0,$

Scenario4) $L_{SR_1} = L_{R_1D} = L_{SR_2} = L_{SR_3} = 1, L_{SD} = L_{R_2D} = L_{R_3D} = 0,$

Scenario5) $L_{SR_1} = L_{R_1D} = L_{SR_2} = L_{R_2D} = 1, L_{SR_3} = L_{R_3D} = L_{SD} = 0,$

As is illustrated in Fig. 5, first two scenarios have identical slopes for high E_{SD}/N_0 values, achieving the full diversity order of $L_{SD}+1+\sum_{i=1}^{3}\left(\min(L_{SR_i},L_{R_iD})+1\right)=4$. The next two scenarios have identical slopes similarly, achieving the full diversity order of $L_{SD}+1+\sum_{i=1}^{3}\left(\min(L_{SR_i},L_{R_iD})+1\right)=5$. The last scenario achieves the highest numerical diversity order of 6, as can be seen from the figure.

Finally, Fig. 6 illustrates SER performance for the D-ZP-OFDM-MMSE, LC-MMSE-ZP-OFDM receiver with error propagation (EP), and the LC-MMSE-ZP-OFDM receiver without EP when $L_{SR_1}=L_{SR_2}=L_{SR_3}=0$, and $L_{SD}=L_{R_1D}=L_{R_2D}=L_{R_3D}=1$. As is illustrated in Fig. 6, the LC-MMSE-ZP-OFDM receiver outperforms the D-ZP-OFDM-MMSE, i.e. 3dB at SER $=10^{-5}$ when having no EP from the feed-forward stage to the feedback stage. Note that with EP, the LC-MMSE-ZP-OFDM receiver outperforms the D-ZP-OFDM-MMSE by 1 dB at SER $=10^{-5}$ as is illustrated in Fig. 6.

As can be concluded from the simulation results that, in dual hop networks, the hop with the smaller diversity order becomes the performance bottleneck.

TABLE I: COMPARISON OF OVERALL COMPUTATIONAL COMPLEXITY

Implementation	Number of Complex Multiplications			Number of Complex Divisions		
	Scenario 1	Scenario 2	Scenario 3	Scenario 1	Scenario 2	Scenario 3
D-ZP-OFDM-MMSE	10728	13224	15720	NONE	NONE	NONE
LC-MMSE-ZP-OFDM	3037	7651	14659	80	80	80

VI. CONCLUSION

In this paper, we propose an efficient iterative receiver for cooperative ZP-OFDM systems. We show that, by incorporating linear processing techniques, our LC-MMSE-ZP-OFDM receiver is able to collect full antenna and multipath diversity gains. We have provided complete complexity analysis, as well as, numerical results to corroborate the analytical studies. Simulation results demonstrate that our LC-MMSE-ZP-OFDM receiver outperforms the cooperative MMSE-ZP-OFDM receiver, while maintaining much lower complexity by avoiding channel dependent matrix inversion. By using linear processing techniques that require minimum computational complexity, the communication power is minimized at no additional hardware cost which makes the LC-MMSE-ZP-OFDM receiver a strong candidate for the energy constrained WSNs.

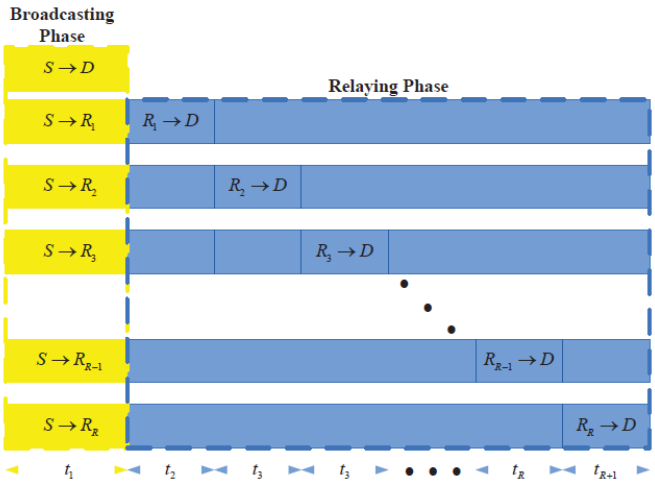

Fig. 1. Transmission block format for multi-relay ZP-OFDM system.

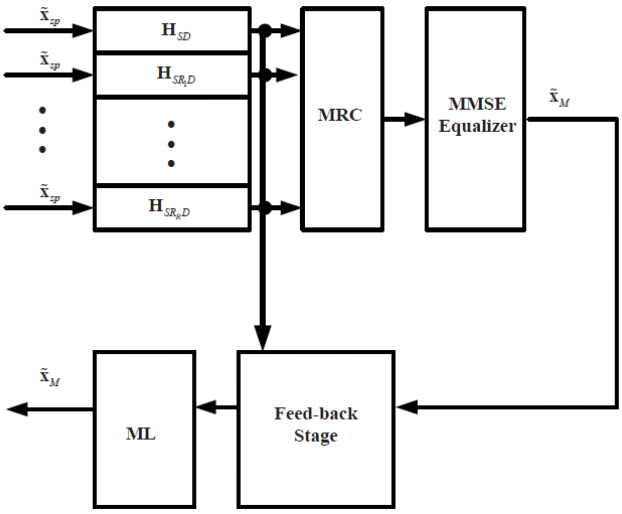

Fig. 2. LC-MMSE-ZP-OFDM receiver's block diagram.

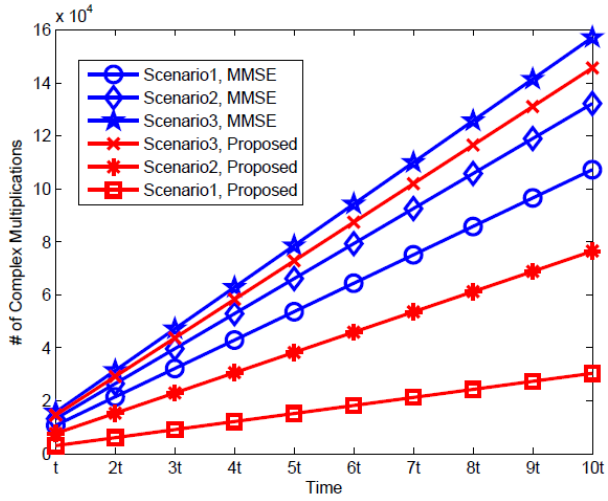

Fig. 3. Computational complexity of the LC-MMSE-ZP-OFDM receiver compared to D-MMSE-ZP-OFDM with $N_R=10$.

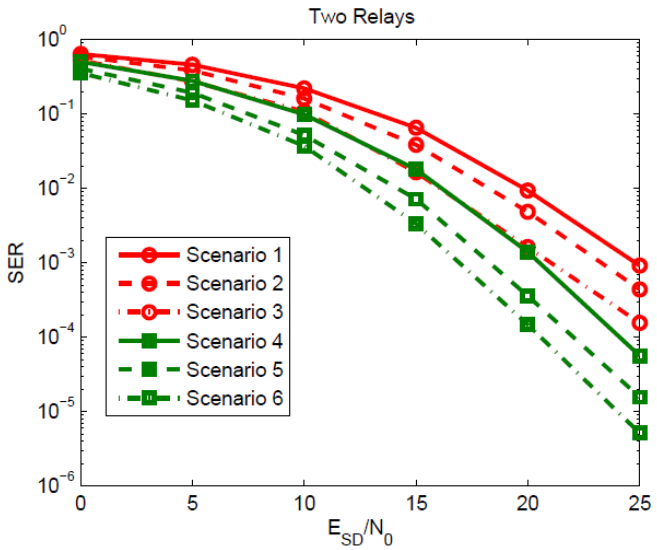

Fig. 4. SER performance of the LC-MMSE-ZP-OFDM receiver for different combinations of channel memory lengths with $N_R = 2$.

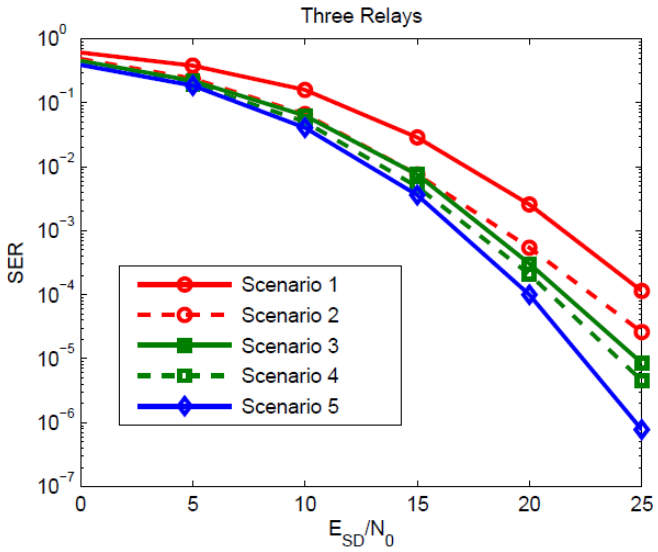

Fig. 5. SER performance of the LC-MMSE-ZP-OFDM receiver for different combinations of channel memory lengths with $N_R = 3$

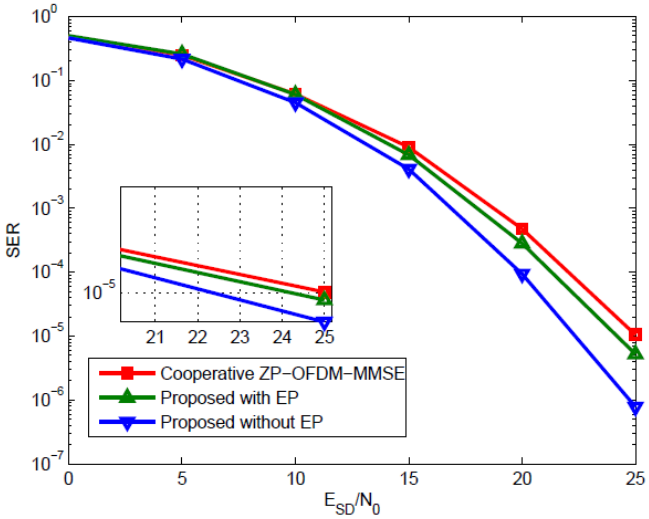

Fig. 6. SER performance of D-MMSE-ZP-OFDM, LC-MMSE-ZP-OFDM with EP, and LC-MMSE-ZP-OFDM without EP.

REFERENCES

[1] Z.Wang and G.B. Giannakis, "Linearly Precoded or Coded OFDM against Wireless Channel Fades?," in *Proceedings of the IEEE Workshop on Signal Processing Advances for Wireless Communications*, Taiwan, China, Mar. 2001.

[2] W. W. Lu, "Compact Multidimensional Broadband Wireless: The Convergence of Wireless Mobile and Access," *IEEE Commun. Mag.*, Nov. 2000, pp. 119-123.

[3] ETSI Normalization Commitee, "Digital Broadcasting Systems for Television, Sound and Data Services; Framing Structure, Channel Coding and Modulation for Digital Terrestrial Television," Norme ETSI, document pr ETS 300 744, European Telecommunications Standards Institute, Sophia-Antipolis, Valbonne, France, 1996.

[4] ANSI T1E1.4 Committee Contribution, "The DWMT: a multicarrier transceiver for ADSL using M-band wavelets," Tech. Rep., ANSI, Mar. 1993.

[5] Broadband Radio Access Networks (BRAN); HIPERLAN Type 2 Technical Specification Part 1-Physical Layer, Eur. Telecommun. Standards Inst. (ETSI), DTS/BRAN030 003-1, 1999.

[6] D. P. Palomar, J. M. Cioffi, and M. A. Lagunas, "Joint Tx-Rx beamforming design for multicarrier MIMO channels: A unified framework for convex optimization," *IEEE Trans. Signal Process*., vol. 51, no. 9, Sep. 2003.

[7] D. Divsalar and M. K. Simon, "Multiple trellis coded modulation (MTCM)," *IEEE Trans. Commun*., vol. 36, pp. 410-419, Apr. 1988.

[8] W. Zou and Y. Wu, "COFDM: an overview," *IEEE Trans. Broadcast*., vol. 41, pp. 1-8, Mar. 1995.

[9] A. J. Viterbj, "Error bounds for convolutional codes and an asymptotically optimum decoding algorithm," *IEEE Trans. Inform. Theory*, vol. IT-13, pp. 260-269, Apr. 1967.

[10] Z. Liu, Y. Xin, and G. B. Giannakis, "Linear constellation precoding for OFDM with maximum multipath diversity and coding gains," *IEEE Trans. Commun*., vol. 51, pp. 416-427, March 2003.

[11] J. Boutros and E. Viterbo, "Signal space diversity: a power- and bandwidth-efficient diversity technique for the Rayleigh fading channel," *IEEE Trans. Inform. Theory*, vol. 44, pp. 1453-1467, July 1998.

[12] A. O. Hero and T. L. Marzetta, "Cutoff rate and signal design for the quasi-static Rayleigh fading space-time channel," *IEEE Trans. Inform. Theory*, vol. 47, pp. 2400-2416, Sept. 2001.

[13] Y. Rong, S. A. Vorobyov, and A. B. Gershman, "Linear block precoding for OFDMsystems based on maximization of mean cutoff rate," *IEEE Trans. Signal Process*., vol. 53, no. 12, pp. 4691-4696, Dec. 2005.

[14] B. Muquet, Z.Wang, G. B. Giannakis, M. de Courville, and P. Duhamel, "Cyclic prefixing or zero padding for wireless multicarrier transmissions?," I*EEE Trans. Commun*., vol. 50, pp. 2136-2148, Dec. 2002.

[15] J. N. Laneman, D. N. C. Tse, and G. W. Wornell, "Cooperative diversity in wireless networks: Efficient protocols and outage behavior," *IEEE Trans. Inform. Theory*, vol. 49, pp. 3062-3080, Dec. 2004.

[16] H. Mheidat, M. Uysal, and N. Al-Dhahir, "Equalization Techniques for Distributed Space-Time Block Codes with Amplify-and-Forward Relaying", *IEEE Trans. Signal Process*., vol. 55, no. 5, part 1, p. 1839-1852, May 2007.

[17] A. Sendonaris, E. Erkip, and B. Aazhang, "User cooperation diversity. Part I. System description," *IEEE Trans. Commun.*, vol. 51, no. 11, pp. 1927-1938, Nov. 2003.

[18] A. Sendonaris, E. Erkip, and B. Aazhang, "User cooperation diversity. Part II. Implementation aspects and performance analysis," *IEEE Trans. Commun*., vol. 51, no. 11, pp. 1939-1948, Nov. 2003.

[19] J. N. Laneman and G. W.Wornell, "Distributed space-time-coded protocols for exploiting cooperative diversity in wireless networks," *IEEE Trans. Inf. Theory*, vol. 49, no. 10, pp. 2415-2425, Oct. 2003.

[20] M. Janani, A. Hedayat, T. E. Hunter, and A. Nosratinia, "Coded cooperation in wireless communications: space-time transmission and

iterative decoding," *IEEE Trans. Signal Process*., vol. 52, no. 2, pp. 362-371, Feb. 2004.
[21] G. Li and H. Liu, "On the capacity of the broadband relay networks," in *Proc. Asilomar Conf. Signals, Syst., Comput.*, Nov. 2004, pp. 1318-1322.
[22] M. Herdin, "A chunk based OFDM amplify-and-forward relaying scheme for 4G mobile radio systems," in *Proc. IEEE Int. Conf. in Commun. (ICC)*, June 2006, pp. 4507-4512.
[23] W. P. Siriwongpairat, A. K. Sadek, and K. J. R. Liu, "Cooperative communications protocol for multiuser OFDM networks," *IEEE Trans. Wireless Commun.*, vol. 7, no. 7, pp. 2430-2435, July 2008.
[24] L. Dai, B. Gui, and L. J. Cimini, "Selective relaying in OFDM multihop cooperative networks," in *Proc. IEEE Wireless Commun. and Networking Conf.*, Mar. 2007, pp. 963-968.
[25] R. U. Nabar, H. Bolcskei, and F.W. Kneubuhler, "Fading relay channels: Performance limits and space-time signal design," *IEEE J. Sel. Areas Comm.*, vol. 22, no. 6, pp. 1099-1109, Aug. 2004.
[26] O-S. Shin, A. Chan, H. T. Kung, and V. Tarokh, "Design of an OFDM co-operative diversity system," *IEEE Trans. Vehicular Tech.*, vol. 56, no. 4, pp. 2203-2215, July 2007.
[27] S. Barbarossa and G. Scutari, "Distributed space-time coding for regenerative relay networks," *IEEE Trans. Wireless Commun.*, vol. 4, no. 5, pp. 2387−2399, Sep. 2005.
[28] Y. Ding and M. Uysal, "Amplify-and-forward cooperative OFDM with multiple-relays: Performance analysis and relay selection methods," *IEEE Trans. Wireless Commun.*, vol. 8, no. 10, pp. 4963-4968, Oct. 2009.
[29] M. Uysal, O. Campolat, and M.M. Fareed, "Asymptotic performance analysis of distributed space-time codes," *IEEE Commun. Lett*., vol.10, no.11, pp. 775-777, Nov. 2006.
[30] I. S. Gradshteyn and I. M. Ryzhik, Table of Integrals, Series and Products. New York: Academic, 2000.
[31] M.T. Heideman and C. Sidney Burrus, "On the number of multiplications necessary to compute a length-2n DFT," *IEEE Trans. Acoust. Speech. Sig. Proc.*, vol. 34, 1986, pp. 91−95.
[32] P. Duhamel and M. Vetterli, "Fast Fourier transforms: a tutorial review and a state of the art," *Signal Processing*, no. 19, 1990, pp. 259−299.
[33] J. M. Cioffi, G. P. Dudevoir,M. V. Eyuboglu, and G. D. Forney, "MMSE decision feedback equalizers and coding: Part I and II," *IEEE Trans. Commun.*, vol. 43, pp. 25822604, Oct. 1995.

Homa Eghbali received the B.Sc. in Electrical Engineering from American University of Sharjah, Sharjah, UAE, in 2009, and the M.Sc. degree in Electrical Engineering from Simon Fraser University, Burnaby, Canada, in 2010. Since June 2010, she has been with the Department of Engineering Science, Simon Fraser University, working towards the Ph.D. degree. Her current research focus is on equalization, multicarrier communication techniques, cooperative communication, and MIMO wireless communication.

Ibrahim Abualhaol received the B.Sc. and the M.Sc. degrees in electrical engineering from Jordan University of Science and Technology, Irbid, Jordan, in 2000 and 2004, respectively, and the Ph.D. degree in electrical engineering from the University of Mississippi, Oxford, MS, in August 2008. He worked as Research Assistant with the Center for Wireless Communication at the University of Mississippi, MS, form Jan 2005 until Aug 2008. From May 2008 to Sep 2009, he worked as Wireless System Engineer with Qualcomm Incorporation and then with Broadcom Corporation at San Diego, CA. He is currently an Assistant Professor at Khalifa University of Science, Technology, and Research at Sharjah, United Arab Emirates. Dr. Abualhaol research interests include OFDM, space–time coding, cooperative networks, and MIMO wireless communications. He is a senior member of IEEE, a member of Phi Kappa Phi, and a member of Sigma Xi.

Sami Muhaidat (S'01-M'07) received the M.Sc. in Electrical Engineering from University of Wisconsin, Milwaukee, USA in 1999, and the Ph.D. degree in Electrical Engineering from University of Waterloo, Waterloo, Ontario, in 2006. From 2003 to 2006, he worked as a Research and Teaching Assistant in Wireless Communication Systems (WiComS) Research Group at the University of Wisconsin. From 2006 to 2008, he was a postdoctoral fellow in the Department of Electrical and Computer Engineering, University of Toronto, Canada. He is currently an Assistant Professor with the School of Engineering Science at Simon Fraser University, Burnaby, Canada. Dr. Muhaidat is an Associate Editor for IEEE Transactions on Vehicular Technology.